FERRITIC AND AUSTENITIC SINTERED STAINLESS STEELS FATIGUE CRACK PROPAGATION RESISTANCE: HYDROGEN EMBRITTLEMENT INFLUENCE

F, Iacoviello, V. Di Cocco
Di.M.S.A.T., Università di Cassino, Cassino (FR), ITALY

ABSTRACT

Stainless steels are widely used in many fields such as chemical, petrochemical, food and nuclear industries and they are characterized by physical, mechanical and corrosion resistance properties that depend on the microstructure and phase transformations: many intermetallic phases, carbides and nitrides precipitate at different tempering temperatures. Sintered stainless steels corrosion resistance and mechanical behavior are worst than that of either cast or rolled or wrought stainless steels: their use is mainly due to their economically attractive production cost and/or to their alternative manufacturing procedure (e.g. duplex stainless steels).
In this work, the fatigue crack propagation resistance of two sintered stainless steels, respectively characterized by an austenitic and a ferritic microstructure, is investigated. Fatigue crack propagation tests are performed both in air and under hydrogen charging conditions, investigating the influence of the stress ratio (R= 0.1; 0.5; 0.75). Fatigue crack propagation micromechanisms are investigated by means of a scanning electron microscope (SEM) fracture surface analysis.
Although the hydrogen physical behaviour is completely different in fcc and bcc structures, both the investigated austenitic and ferritic sintered stainless steels are susceptible to be embrittled by the hydrogen charging process, for all the investigated stress ratio values. SEM fracture surface analysis allows to identify different fatigue crack propagation mechanisms that are influenced both by the loading conditions (either ΔK and R values), by the steel microstructure and by the test environment.

1 INTRODUCTION

Stainless steels obtained by means of the "traditional" metallurgy are susceptible to failure by hydrogen embrittlement under certain combinations of hydrogen charging, temperature and stress (Gibala [1]). Hydrogen sources could be related to a galvanic coupling with less noble metals (e.g. carbon steels), from cathodic protection, from welding operations and from localized corrosion. Considering that stainless steels are attractive materials for many applications (e.g. petrochemical industry, chemical and nuclear plants, marine environment, desalination etc.) and that they could be considered as critical with respect to the hydrogen embrittlement problem, it is necessary to assess their susceptibility to this damaging mechanism (Chêne [2]). Stainless steels are sometimes characterized by considerable difficulties from the manufacturing point of view (e.g. austenitic-ferritic duplex stainless steels , Datta [3]), and powder metallurgy offers an excellent alternative to produce these steels. Furthermore, sintered stainless steels allow a decreasing of the production costs, especially when a large number of identical pieces, usually characterized by a small size and a complex geometry, is produced (Otero [4]). Sintered duplex stainless steels are obviously characterized by the presence of micropores that depend on the sintering procedures (powders, sintering temperature and duration, etc.). These defects could influence the hydrogen embrittlement susceptibility, especially considering a crack growing under fatigue loading conditions.

Hydrogen is available on a metal surface from various sources. Considering an aqueous environment, all the corrosion mechanisms imply the existence of cathodic reactions and the possible hydrogen adsorption on metal surface (Chêne [5]):

$$H^+ + e^- + M \leftrightarrow MH_{ads} \text{ (acid environments)}$$

$$H_2O + e^- + M \leftrightarrow MH_{ads} + OH^- \text{ (alkaline environments)}$$

Then, adsorbed hydrogen contained in MH_{ads} species could be:

- absorbed according to: $MH_{ads} \leftrightarrow MH_{abs}$
- recombined in molecular form according to: $MH_{ads} + MH_{ads} \leftrightarrow H_2 + 2M$
- desorbed according to: $MH_{ads} + H^+ + e^- \leftrightarrow H_2 + M$

The distribution of the absorbed hydrogen (MH_{abs}) on the crack surface is influenced by many factors as the electrochemical environment at the crack tip (potential, pH, species concentrations, O_2, etc) and the kinetics of the involved reactions. Transport rate of absorbed hydrogen from the crack surface into the material depends on the hydrogen physical behaviour in metals. The main aspects of this behaviour are (Johnson [6], Bernstein [7]):

- hydrogen solubility;
- hydrogen diffusivity;
- hydrogen trapping.

Both hydrogen solubility and diffusivity depend on the microstructure, on the temperature (at room temperature, the coefficient of hydrogen diffusion, D_H, in body centered cubic lattice ranges between about 10^{-9} cm^2s^{-1} and about 10^{-6} cm^2s^{-1}; these D_H values can be obtained in a face centered cubic lattice only for higher temperatures, between 200°C and 600°C, Welding Institute [8]), on the stresses state and, finally, on the presence of lattice defects as vacancies, alloying elements, dislocations interfaces, microvoids and grain boundaries. External or internal stresses influence the hydrogen solubility and diffusivity in metals, depending on the consequent strain level. An elastic deformation field implies a solubility increase or a decrease respectively corresponding to a tensile or a compression stress state, while diffusion coefficients are not influenced by an elastic deformation field. A plastic deformation field implies a strong increase of the dislocations density: as a consequence, an evident increase of the hydrogen concentration is obtained according to a "trapping" mechanism. The so called "hydrogen trapping" phenomenon (Pressouyre [9, 10]) could be defined as the ability of hydrogen in solid solution to interact with all the microstructural defects, influencing both hydrogen physical behaviour (diffusivity and solubility) and metals mechanical behaviour (i.e. hydrogen induced crack or hydrogen embrittlement). Different traps classifications were proposed, depending on:

- traps position (internal or external);
- traps origin (connected to electric or chemical or elastic interactions);
- traps physical characteristics ("attractive" traps as electrical or stress fields or temperature gradients; "physical" traps as high angle grain boundaries or incoherent particle matrix or voids; "mixed" traps as edge dislocations);
- hydrogen-trap interaction energy, defining the concept of "reversible" or "irreversible" trap, that depends on the temperature ("reversible" traps release hydrogen continuously with the temperature increasing, while irreversible ones do so after a critical temperature is reached);
- traps dimension (zero-dimensional as interstitials or vacancies, mono-dimensional as dislocations, bi-dimensional as phases interfaces or grain boundaries, and three-dimensional as micropores).

Considering all the physical, chemical, metallurgical and mechanical parameters that influence the hydrogen charging, diffusion, solubility and trapping in metals, many hydrogen embrittlement models are available, but no one is applicable to all the possible conditions (Coudreuse [11]).

The analysis of the fatigue crack propagation resistance in air and under hydrogen charging conditions of sintered stainless steels should take into account both the microstructure (austenitic or ferritic grains) and the microvoids presence.

2 MATERIALS AND EXPERIMENTAL PROCEDURES

Two sintered stainless steels are obtained considering AISI 316 LHC and AISI 434 LHC stainless steels powders (table 1). Sintering was performed at 1250°C, under vacuum, for 1 hour.

Table 1: Stainless steels powders chemical compositions (wt%).

	C	Mo	Ni	Mn	Cr	Si	Fe
AISI 316 (ρ = 7.08 g/cm^3)	0.019	2.28	12.75	0.17	16.3	0.87	Bal.
AISI 434 (ρ = 7.16 g/cm^3)	0.016	1.03	-	0.18	16.57	0.70	Bal.

Fatigue tests are perfomed using 10.5 mm thick CT (Compact Type) specimens, with the notch obtained via electroerosion. Sintered stainless steels fatigue crack propagation resistance areinvestigated according to E647 ASTM standard (ASTM [12]), using a computer controlled (100 kN) servohydraulic testing machine in constant load amplitude conditions, with a sinusoidal waveform. Tests are performed at room temperature, both in air, with a loading frequency of 30 Hz, and under hydrogen charging conditions (0.5 M H_2SO_4 + 0.01 M KSCN aqueous solution; applied potential = -0.7 V/SCE) with a loading frequency of 1 Hz, considering three different stress ratio values (e.g. $R = P_{min}/P_{max}$ equal to 0.1, 0.5 and 0.75). Crack lengths are measured using a compliance method with a double cantilever crack mouth gauge and are controlled using an optical method with a 40x magnification. da/dN-ΔK experimental results are interpolated considering the Paris law in the stage II of III (Paris [13]):

$$da/dN = C\,\Delta K^m \quad (1)$$

where *C* and *m* are interpolation parameters. These parameters depend on material, structural state mechanical properties and environmental test conditions (Iost [14]).

Main crack propagation micromechanisms are investigated by means both of a scanning electron microscope (SEM Philips with EDX) fracture surfaces analysis. Furthermore, an optical microscope (LOM, x200) fatigue crack path analysis is conducted with the same procedure followed in Iacoviello [15].

3 RESULTS

Fatigue crack propagation results are shown in figures 1 and 2. Ferritic sintered stainless steel fatigue crack propagation (figure 1) is characterized by the decrease of the threshold values (ΔK_{th}) and the increase of the crack growth rates with the increasing of the stress ratio (e.g. R). This result is obtained both considering air laboratory conditions and under hydrogen charging conditions. Differences between fatigue crack growth values under hydrogen charging conditions (e.g. $(da/dN)_H$) and in air (e.g. $(da/dN)_A$) decrease with the increase of ΔK values. On the other hand, the stress ratio influence is almost negligible. Austenitic sintered stainless steel (figure 2) is characterized by an evident influence of the stress ratio on the da/dN-ΔK results that is analogous to the ferritic one, but differences between $(da/dN)_H$ and $(da/dN)_A$ are lower: these differences increase with the stress ratio, and, similarly to the ferritic steel, decrease with the increase of ΔK values. Paris relationship interpolation coefficients *C* and *m* are influenced by both the microstructure, and the loading and the test environment conditions (figure 3). For each investigated stainless steel and considered loading condition, *m* values obtained in air (e.g. m_A) are systematically higher than the corresponding values obtained under hydrogen charging conditions

(e.g. m_H). Considering that m parameter corresponds to the slope of the experimental points in the log(da/dN)-log(ΔK) diagram, that differences between m_A and m_H are more evident for the ferritic sintered stainless steel with respect to the austenitic one and that, for both the investigated sintered stainless steels, differences between m_A and m_H depend on the stress ratio, it follows that the hydrogen embrittlement suscesceptibility of the ferritic sintered stainless steel is higher with respect to the austenitic one, with the hydrogen embrittlement susceptibility of the austenitic sintered stainless steel that is, however, not negligible.

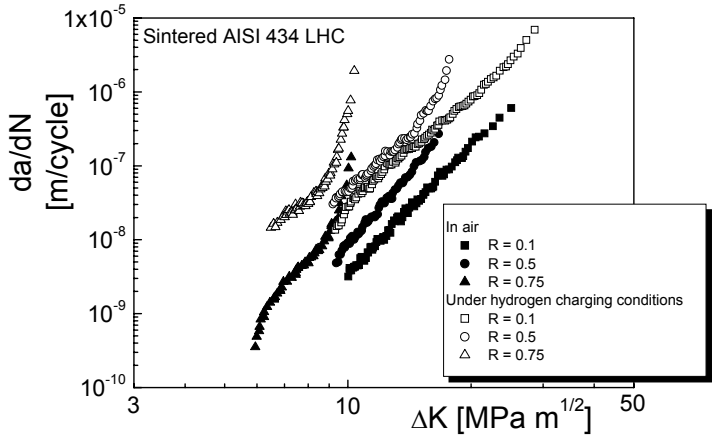

Figure 1: Ferritic sintered stainless steel fatigue crack propagation (air and hydrogen charging conditions).

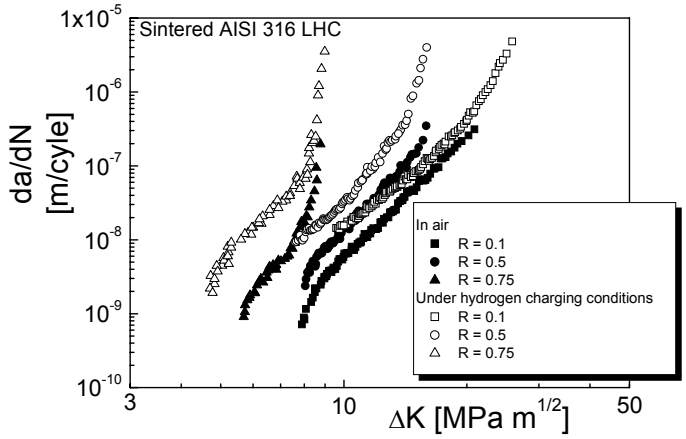

Figure 2: Austenitic sintered stainless steel fatigue crack propagation (air and hydrogen charging conditions).

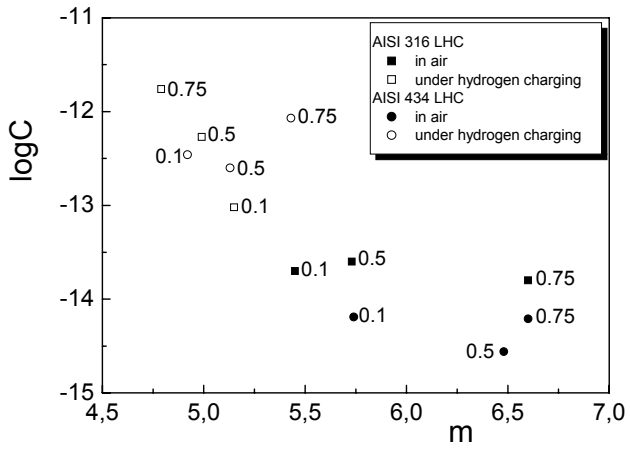

Figure 3: Paris relationship *C* and *m* interpolation parameters for the investigated sintered stainless steels, in air and under hydrogen charging conditions (different R values).

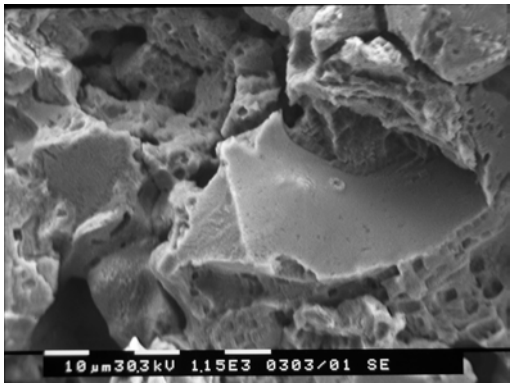

Figure 4: SEM fracture surface analysis (Ferritic stainless steel; hydrogen charge; R = 0.75; $\Delta K = 8$ MPa$\sqrt{m}$)

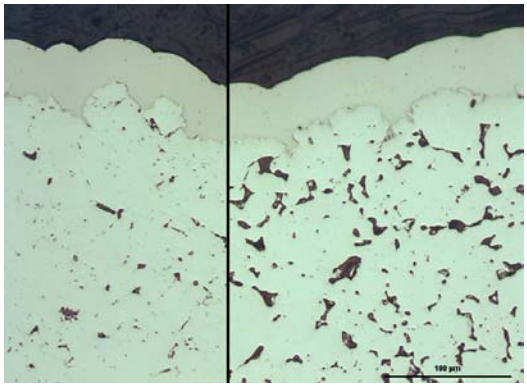

Figure 5: LOM crack profile analysis: micropores distribution (austenitic stainless steel; R = 0.1; $\Delta K = 10$ MPa$\sqrt{m}$)

SEM fracture surfaces analysis and LOM fracture profiles analysis allow identifying the influence of the steels microstructure on the fatigue crack propagation under hydrogen embrittlement conditions. The hydrogen embrittlement of the ferritic sintered stainless steel implies an increase of the importance of cleavage (figure 4, crack propagates form left to right). This is due to the high susceptibility to hydrogen embrittlement that characterizes the bcc lattice, due to the high diffusion coefficients and low solubility values, also at room temperature. Austenitic sintered stainless steel is also characterized by evident hydrogen embrittlement susceptibility, although the hydrogen diffusion coefficients are very low at room temperature. This is probably due to the micropores presence: in fact, in the region around the crack, LOM analysis shows an increase of micropores dimension for the steel under hydrogen charging condition (figure 5: crack profile and micropores distribution in air, on the left, and under hydrogen charging conditions, on the right). Hydrogen diffuses very slowly in the fcc lattice, but, when it finds a micropore, it is trapped very deeply. It

follows an increase of the hydrogen internal pressure, connected to the molecular hydrogen recombination, with a consequent crack growing due to the high hydrogen pressures (Coudreuse [11]).

4 CONCLUSIONS

In this work, the fatigue crack propagation resistance of two sintered stainless steels, respectively characterized by an austenitic and a ferritic microstructure, is investigated both in air and under hydrogen charging conditions. Hydrogen embrittlement micromechanisms depend on the steels microstructure and on the micropores presence: ferritic sintered stainless steel hydrogen embrittlement is characterized by the increasing of the importance of cleavage. Austenitic sintered stainless steel is characterized by the interaction of the hydrogen with micropores. The following embrittlement micromechanism probably implies a molecular hydrogen recombination, with a consequent crack growing due to the high hydrogen pressures inside micropores.

5 REFERENCES

[1] Gibala R., Kumnick A.J., Hydrogen trapping in iron and steels, Hydrogen embrittlement and stress corrosion cracking, edited by R. Gibala and R.F. Hehemann, 61-78, 1984.

[2] Chêne J., Aucouturier M., Arnould-Laurent R., Tison P., Fidelle J.P., Hydrogen transport by dislocations and hydrogen embrittlement in stainless steels, 3rd International Conference on the effect of hydrogen on behaviour of materials, Jackson Lake, Wyoming USA, 26-31, 1980.

[3] Datta P., Upadhyaya G.S., Sintered duplex stainless steels from premixes of 316L and 434L powders, Materials Chemistry and Physics, 67, 234-242, 2001.

[4] Otero E., Pardo A., Utrilla M.V., Sàenz E., Alvarez J.F., Corrosion behaviour of AISI 304L and 316L prepared by powder metallurgy in the presence of sulphuric and phosphoric acid, Corrosion Science, 40, 8, 1421-1434, 1998.

[5] Chêne J., Brass A.M., Interaction Hydrogène-Métal en relation avec le processus de corrosion sous contrainte, Corrosion sous contrainte, Edited by D. Desjardins and R. Oltra, Bombannes, 159-210, 1990 .

[6] Johnson H.H., Overview on hydrogen degradation phenomena, Hydrogen embrittlement and stress corrosion cracking, edited by R. Gibala and R.F. Hehemann, 3-27, 1984.

[7] Bernstein I.M., Thompson A.W., The role of microstructure in hydrogen embrittlement, Hydrogen embrittlement and stress corrosion cracking, edited by R. Gibala and R.F. Hehemann, 135-152, 1984.

[8] The Welding Institute, Welding steels without hydrogen cracking, WI Publications, 1978.

[9] Pressouyre G. M., Bernstein I. M., A quantitative analysis of hydrogen trapping, Metallurgical Transactions A, 9A, 1571-1580, 1978.

[10] Pressouyre G.M., A classification of hydrogen traps, Metallurgical Transactions A, 10A, 1571-1573, 1979.

[11] Coudreuse L., Fragilisation par l'hydrogène et corrosion sous contrainte, Corrosion sous contrainte, Edited by D. Desjardins and R. Oltra, Bombannes, 397-424, 1990.

[12] ASTM Standard test Method for Measurements of fatigue crack growth rates (E647-93), Annual Book of ASTM Standards,1993, 0301, American Society for Testing and Materials.

[13] Paris P.C., The trend of Engineering at the University of Washington, 1961, 13(1), 9.

[14] Iost A., The effect of load ratio on the m-lnC relationship, Int. J. of Fatigue, 13, 25-32, 1991

[15] Iacoviello F., Di Cocco V., Cavallini M., Marcu T., Molinari A., Fatigue crack paths in sintered duplex stainless steels, International Conference on Fatigue Crack Paths, Parma, Italy, 15, 2003.